Modeling Anisotropy and Steady State Creep in a Rotating Disc of Al-SiCp having Varying Thickness

Vandana and S.B. Singh

Abstract: *The analysis of steady state creep in a rotating disc made of Al-SiCp composite having variable thickness has been carried using Sherby's constitutive model. The creep parameters have been evaluated using the available experimental results in the literature using regression analysis. Three variations in the thickness (constant, linearly and hyperbolic varying thickness) of the disc have been considered while keeping other material parameters same. The change in the radial stress in all the three cases is not significant while the tangential stress is changed with the change in the values of anisotropic constants. The tangential strain rates are highest at the inner radius of the disc and then decreases towards the outer radius of the discs. The radial strain rate which is compressive in nature becomes tensile in middle of the disc for some specific values of anisotropic constants. The study reveals that the anisotropy and thickness profile has a significant effect on the creep behavior of rotating disc. Thus for the safe design of the rotating disc the effect of anisotropy and profile should be taken care of.*

Keywords: *Modeling, Composites, Rotating Disc, Steady Strain Creep Rate*

1 INTRODUCTION

Theoretical investigation of the stresses in solid and annular discs rotating at high speeds have received widespread attention due to a large number of applications in engineering like turbine motors, flywheels, gears, shrink fits etc. They are usually operated at relatively higher angular speed and high temperature. Therefore the prediction of long term steady state creep deformation is very important for these applications.

Turbine discs are usually designed by decreasing the thickness with increasing radius. This feature introduced a disc with varying thickness for using the material of disc more effectively. It is shown that the analysis of creep behavior in a disc with varying thickness is complicated than that of a disc with constant thickness.

Wahl et al. [1] have theoretically studied steady state creep described creep behavior by a power function in a rotating turbine disc made of 12% chromium steel at 1000° F using Von Mises and Tresca yield criteria and validated their results experimentally. Ma [2,3] have carried out creep analysis of solid disc. The analysis shows that by changing the profile of disc, stress is quite different from those observed in a disc of constant thickness. Arya and Bhatnagar [5] have carried out creep analysis of orthotropic rotating disc using constitutive equations and a time hardening law. It is reported that the tangential stress at any radius and the tangential strain rate at the inner radius decrease with increasing anisotropy of the material. Nieh et al. [6] has shown that an aluminum based composite containing silicon carbide whisker has better creep resistance compared to the base aluminum alloy. Jerzy Biakiewicz [7] has presented a theoretical analysis of the finite strains in a rotating discs followed by damage and creep rupture front motion as described by Kachanov's hypothesis. The creep is represented by the generalized Norton-Odqvist law. Bhatnagar et al. [9] have performed steady state creep analysis of orthotropic rotating discs having constant thickness, linearly varying thickness and hyperbolically varying thickness. They have used Norton's power law to describe creep behavior of the disc material. Pandey et al. [10] have studied the steady-state creep behavior of Al–SiCp composites under uniaxial loading condition in the temperature range between 623K and 723K for different combinations of particle size and volume fraction of reinforcement and found that the composite with finer particle size has better creep resistance than that containing coarser ones. Gupta et al. [11] have obtained creep stresses and strain rates in thin rotating disc having variable

Dr S.B. Singh, is Professor and Head, Department of Mathematics, Punjabi University, Patiala-147002, INDIA, Email ID: sbsingh69@yahoo.com. His research interests are Mathematical Modeling in Composite Material and Optimization Techniques. He has published 50 research papers in Journals/Conference Proceedings. He was awarded Khosla Gold Medal by I.I.T. Roorkee for his outstanding research contributions.

Ms.Vandana is a Ph.D. student in the Department of Mathematics, Punjabi University, India, Punjab, Patiala-147002. vaggarwal2584@gmail.com.

thickness and variable density by using Seth's transition theory. It is observed that a rotating disc whose density and thickness ratio decreases radially is on the safer side of the design in comparison to a flat disc having variable density. Singh and Ray [12] have analyzed steady state creep in an anisotropic composite disc showing Bauschinger effect, using Norton's power law and newly proposed yield criterion. This yield criterion results in significant changes in the tangential stress distribution but similar radial stress distributions in disc with residual stress compared to those obtained in a similar disc without residual stress following Hill's yield criterion. The presence of tensile residual stress in the disc is observed to increase the creep rate significantly compared to that in a similar anisotropic disc without residual stress. Orcan and Eraslan [13] investigated the distribution of stress, displacement and plastic strain in a rotating elastic–plastic solid disk of variable thickness in a power function. The analysis is based on Tresca's yield condition, its associated flow rule and linear strain hardening material behavior. By employing a variable thickness disc the plastic limit angular velocity increases and the magnitude of stresses and deformations in the disc reduces. Gupta et al. [14] have analyzed steady state creep in isotropic aluminum silicon carbide particulate rotating disc. The creep behavior has been described by Sherby's law. It is observed that the tangential as well as radial stress distribution in the disc do not vary significantly for various combinations of material parameters and operating temperatures. The tangential as well as radial strain rates in the disc reduces significantly with reducing particle size, increasing particle content and decreasing operating temperature. Jahed et al. [15] observed that the use of variable thickness disc helps in minimizing the weight of disc in aerospace applications. There are numerous applications for gas turbine discs in the aerospace industry such as in turbojet engines. These discs normally work under high temperatures while subjected to high angular velocities. Minimizing the weight of such items in aerospace applications results in benefits such as low dead weights and lower costs. Baykara [16] explained the stress concentration factors at a small circular hole in a large sheet of plastic anisotropy, subjected to equi-biaxial tension. In this analysis an orthotropic yield function suggested by Hill and approximate solution technique developed by Durban are used. Numerical results for aluminum and copper sheets are presented. Singh and Ray [17] have performed creep analysis in an anisotropic 6061Al-20Wt% SiCw composite disc rotating at 15,000 rpm and undergoing steady state creep at 561K following Norton's power law. The effect of anisotropy induced presumably by processing or inhomogeneous distribution of reinforcements has been investigated. The presence of anisotropy leads to significant reduction in the tangential and radial strain rates over the entire disc and helps in restraining creep response both in the tangential and in the radial directions. Rattan et al. [18] have reported that the creep exponent should be taken as 8. Chamoli et al. [19] have studied the effect of anisotropy on the stress and strain rates and concluded that the anisotropy of the material has a significant effect on the creep of a rotating disc.

Keeping in view, all the above studies for a disc of constant thickness, an effort has been made to study effect of anisotropy on a rotating composite disc with varying thickness by taking creep exponent 8. The volume of all the discs is kept the same. Steady state creep has been analyzed using the Sherby's constitutive model

2. ASSUMPTIONS

For the purpose of analysis the following assumptions are made:

1. Material of disc is orthotropic and incompressible
2. Elastic deformations are small for the disc and therefore they can be can be neglected as compared to creep deformation.
3. Axial stress in the disc may be assumed to be zero as thickness of disc is assumed to be very small compared to its diameter.
4. The composite shows a steady state creep behavior , which may be described by following sherby's law:

$$\dot{\bar{\varepsilon}} = A_s \left(\frac{\bar{\sigma} - \sigma_0}{E} \right)^n$$

where,

$$A_s = \frac{A D_\lambda \lambda^3}{|b_r|^5}$$

where $\dot{\bar{\varepsilon}}$, $\bar{\sigma}, n$, σ_0, A, D_λ, λ, b, E be the effective strain rate, effective stress, the stress exponent, threshold stress, a constant, lattice diffusivity, the sub grain size, the magnitude of burgers vector , Young's modulus.

The above equation may be expressed as

$$\dot{\bar{\varepsilon}} = \left(M \left(\bar{\sigma} - \sigma_0 \right) \right)^n \quad (1)$$

where,

$M = \frac{A_s^{1/n}}{E}$ is Creep Parameter.

5. Material of disc yield according to Hill's Criterion for anisotropic material as given by

$$\bar{\sigma} = \left\{ \frac{1}{(G+H)} \left[F(\sigma_\theta - \sigma_z)^2 + G(\sigma_z - \sigma_r)^2 + H(\sigma_r - \sigma_\theta)^2 \right] \right\}^{1/2}$$

where *F*, *G* and *H* are anisotropic constants. $\bar{\sigma}$ be the effective stress. For biaxial state of stress, the effective stress is,

$$\bar{\sigma} = \left\{ \frac{1}{(G+H)} \left\{ F\sigma_\theta^2 + G\sigma_r^2 + H(\sigma_r - \sigma_\theta)^2 \right\} \right\}^{1/2} \quad (2)$$

In Particle reinforced composite, the material parameters m and σ_0 depend on the particle size and the percentage of dispersed particles apart from the temperature, have been obtained by using the experimental results of Pandey et al. [10].

The following regression equations have been extracted from the available experimental results,

$$m = e^{-35.38} P^{0.2077} T^{4.98} V^{-0.622}$$

$$\sigma_0 = -0.03507P + 0.01057T + 1.00536V - 2.11916$$

3. FUNDAMENTAL RELATIONS

Consider a thin orthotropic composite disc of 6061 Al-SiC$_p$ of density ρ and rotating at a constant angular speed ω radian/sec. The thickness of the disc is assumed to be h and a and b be inner and outer radii of the disc respectively. Let I and I_0 be the moment of inertia of the disc at inner radius a and outer radius r and b respectively. A and A_0 be the area of cross section of disc at inner radius a and outer radius r and b respectively. Then

$$I = \int_a^r h\, r^2 dr, \qquad I_0 = \int_a^b h\, r^2\, dr$$

$$A = \int_a^r h\, dr, \qquad A_0 = \int_a^b h\, dr \quad (3)$$

$$\sigma_{\theta\, avg} = \frac{1}{A_0} \int_a^b h\, \sigma_\theta\, dr. \quad (4)$$

The constitutive equations for an anisotropic disc under multiaxial stress condition are given as,

$$\dot{\varepsilon}_r = \frac{\dot{\bar{\varepsilon}}}{2\bar{\sigma}} \{(G+H)\sigma_r - H\sigma_\theta - G\sigma_z\} \quad (5)$$

$$\dot{\varepsilon}_\theta = \frac{\dot{\bar{\varepsilon}}}{2\bar{\sigma}} \{(H+F)\sigma_\theta - F\sigma_z - H\sigma_r\} \quad (6)$$

$$\dot{\varepsilon}_z = \frac{\dot{\bar{\varepsilon}}}{2\bar{\sigma}} \{(F+G)\sigma_z - G\sigma_r - F\sigma_\theta\} \quad (7)$$

where F, G and H are anisotropic constants of the material. $\dot{\varepsilon}_r$, $\dot{\varepsilon}_\theta$, $\dot{\varepsilon}_z$ and σ_r, σ_θ, σ_z are the strain rates and the stresses respectively in the direction r, θ and z. $\dot{\bar{\varepsilon}}$ be the effective strain rate and $\bar{\sigma}$ be the effective stress.

4. ANALYSIS

Using Eqs. (1) and (2), Eq. (5) can be rewritten as,

$$\dot{\varepsilon}_r = \frac{d\dot{u}_r}{dr} = \frac{\sqrt{F(G+H)} \left[\left(\frac{G}{F} + \frac{H}{F} \right) x - \frac{H}{F} \right] \left[M(\bar{\sigma} - \sigma_0) \right]^8}{2 \left[\left(\frac{G}{F} + \frac{H}{F} \right) x^2 - 2\frac{H}{F} x + \left(\frac{G}{F} + \frac{H}{F} \right) \right]^{1/2}} \quad (8)$$

where,

$$x(r) = \frac{\sigma_r}{\sigma_\theta}$$

Similarly from Eq. (6),

$$\dot{\varepsilon}_\theta = \frac{\dot{u}_r}{r} = \frac{\sqrt{F(G+H)} \left[\left(1 + \frac{H}{F} \right) - \frac{H}{F} x \right] \left[M(\bar{\sigma} - \sigma_0) \right]^8}{2 \left[\left(\frac{H}{F} + \frac{G}{F} \right) x^2 - 2\frac{H}{F} x + \left(1 + \frac{H}{F} \right) \right]^{1/2}} \quad (9)$$

$$\dot{\varepsilon}_z = -(\dot{\varepsilon}_r + \dot{\varepsilon}_\theta) \quad (10)$$

Dividing (8) by (9),

$$\phi(r) = \frac{\left(\frac{G}{F} + \frac{H}{F} \right) x - \frac{H}{F}}{\left(1 + \frac{H}{F} \right) - \frac{H x}{F}} \quad (11)$$

where,

$$\phi(r) = \frac{d\dot{u}_r}{dr} \cdot \frac{r}{\dot{u}_r}$$

$$\Rightarrow \quad \frac{d\dot{u}_r}{\dot{u}_r} = \frac{\phi(r)}{r} dr$$

Integrating and taking limit a to r on both sides,

$$\dot{u}_r = \dot{u}_{r_i} \exp. \int_a^r \frac{\phi(r)}{r}\, dr \quad (12)$$

Dividing Eq. (12) by r and equated to Eq. (9),

$$\bar{\sigma} - \sigma_0 = \frac{(\dot{u}_{r_i})^{1/8}}{M}\,\psi(r) \qquad (13)$$

where,

$$\psi(r) = \left\{ \frac{2}{r} \cdot \frac{\left[\left(\frac{H}{F}+\frac{G}{F}\right)x^2 - \frac{2Hx}{F} + \left(1+\frac{H}{F}\right)\right]^{1/2}}{\sqrt{F(G+H)}\left[\left(1+\frac{H}{F}\right)-\frac{H}{F}x\right]} \exp.\int_a^r \frac{\varphi(r)dr}{r} \right\}^{1/8}$$

(14)

Substituting $\bar{\sigma}$ from Eq. (2) to Eq.(13), it gives,

$$\left\{\left(\frac{F}{G+F}\right)\left[\left(\frac{G}{F}+\frac{H}{F}\right)x^2 - 2\frac{H}{F}x + \left(\frac{H}{G}+1\right)\right]\right\}^{1/2} \sigma_\theta - \sigma_0 = \frac{\left(\dot{u}_{r_i}\right)^{1/8}}{M}\psi(r)$$

$$\Rightarrow \quad \sigma_\theta = \frac{\left(\dot{u}_{r_i}\right)^{1/8}}{M}\,\psi_1(r) + \psi_2(r) \qquad (15)$$

$$\Rightarrow \quad \psi_1(r) = \frac{\psi(r)}{\left\{\left(\frac{F}{G+H}\right)\left[\left(\frac{G}{F}+\frac{H}{F}\right)x^2 - 2\frac{H}{F}x + \left(1+\frac{H}{F}\right)\right]\right\}^{1/2}} \qquad (16)$$

$$\psi_2(r) = \frac{\sigma_0}{\left\{\left(\frac{F}{G+H}\right)\left[\left(\frac{G}{F}+\frac{H}{F}\right)x^2 - 2\frac{H}{F}x + \left(1+\frac{H}{F}\right)\right]\right\}^{1/2}} \qquad (17)$$

5. EQUATION OF EQUILIBRIUM

The equation of equilibrium for a rotating disc with varying thickness can be written as,

$$\frac{d}{dr}(r\,h\,\sigma_r) - h\sigma_\theta + \rho\omega^2 r^2 h = 0 \qquad (18)$$

Integrating Eq. (18) within limits a to b and using Eqs. (3) and (4),

$$\sigma_{\theta_{avg}} = \frac{1}{A_0}\rho\omega^2 I_0 \qquad (19)$$

Substituting σ_θ from Eq. (15) into (4),

$$\frac{\left(\dot{u}_{r_i}\right)^{1/8}}{M} = \frac{A_0\ \sigma_{\theta_{avg}} - \int_a^b \psi_2(r).\,hdr}{\int_a^b \psi_1(r).\,hdr} \qquad (20)$$

Using Eq. (19) and (20), Eq. (15) becomes,

$$\sigma_\theta = \frac{\psi_1(r)\left[\rho\omega^2 I_0 - \int_a^b \psi_2(r).\,hdr\right]}{\int_a^b \psi_1(r).hdr} + \psi_2(r) \qquad (21)$$

Integrating Eq. (18) within limits a to r and use Eq.(3),

$$\sigma_r = \frac{1}{r.h}\left[\int_a^r \sigma_\theta\,.h\,dr - \rho\omega^2 I\right] \qquad (22)$$

Thus the tangential stress σ_θ and radial stress σ_r are determined by Eqs. (21) and (22). Then strain rates $\dot{\varepsilon}_r$, $\dot{\varepsilon}_\theta$ and $\dot{\varepsilon}_z$ calculated from equations (5), (6) and (7).

(5.1) DISCS WITH LINEARLY VARYING THICKNESS

The thickness h is assumed to be of the form

$$h = h_b + 2c\,(b - r),$$

and

$$h_a = h_b + 2c\,(b - a)$$

where c is the slope of a disc and the values of c appearing in above equation are calculated as 0.002859.

Using expression, the Eq. (3) becomes,

$$A = (r-a)\left[h_b + c\,(2b - r - a)\right]$$

$$A_0 = (b-a)\left[h_b + c\,(b-a)\right]$$

$$I_0 = \frac{h_b}{3}(b^3 - a^3) + \frac{2cb}{3}(b^3 - a^3) - \frac{c}{2}(b^4 - a^4)$$

$$I = \frac{h_b}{3}(r^3 - a^3) + \frac{2cb}{3}(r^3 - a^3) - \frac{c}{2}(r^4 - a^4)$$

(5.2) DISCS WITH HYPERBOLIC VARYING THICKNESS

The thickness h can be written in the form $h = c\,r^m$ where c and m are constants and the values of c and m appearing in above equation are calculated as 31.26 and - 0.74 respectively.

Using the expression for thickness, the Eq. (3) becomes,

$$A = c\left(\frac{r^{m+1} - a^{m+1}}{m+1}\right), \qquad A_0 = c\left(\frac{b^{m+1} - a^{m+1}}{m+1}\right)$$

$$I = c\left(\frac{r^{m+3} - a^{m+3}}{m+3}\right), \qquad I_0 = c\left(\frac{b^{m+3} - a^{m+3}}{m+3}\right)$$

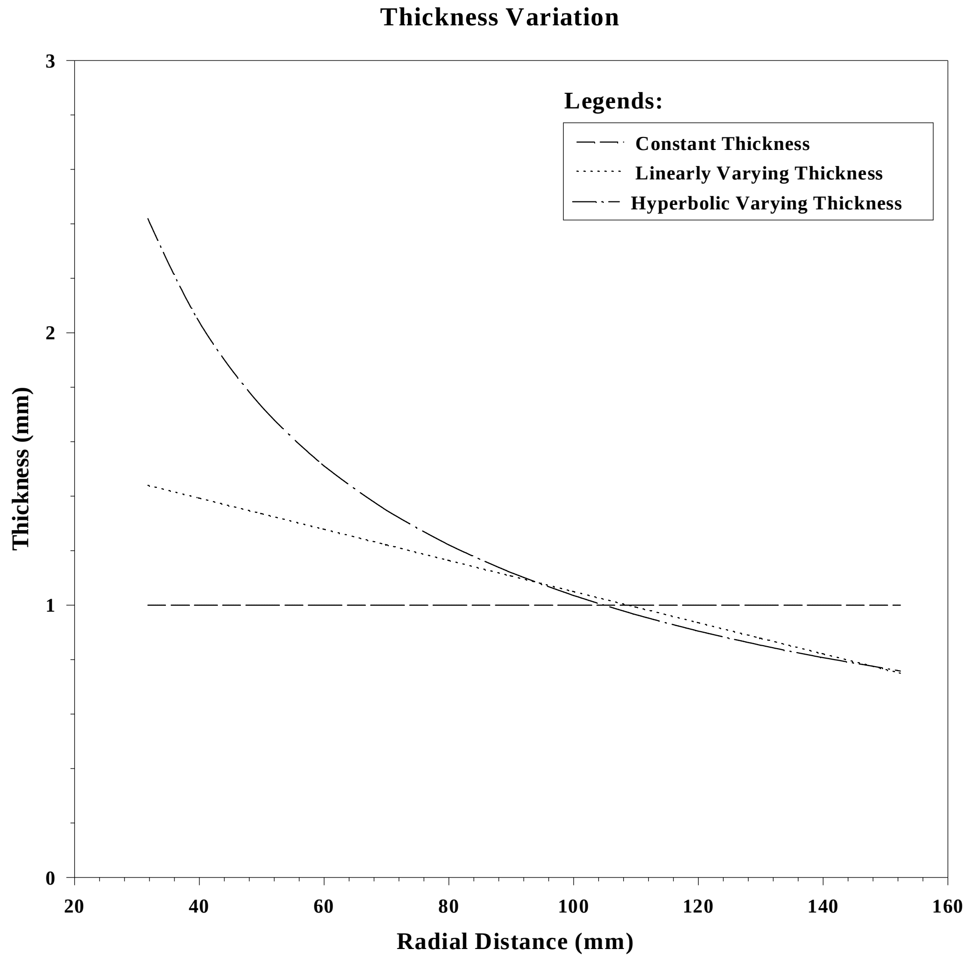

Figure 1: Variation of disc thickness with radial distance for different discs.

6. SOLUTION PROCEDURE

The stress distribution is evaluated from the above analysis by iterative numerical scheme of computation. In the first iteration, it is assumed that $\sigma_\theta = \sigma_{\theta_{avg}}$ over the entire disc radii. Substituting $\sigma_{\theta_{avg}}$ for σ_θ in Eq. (22) the first approximation value of σ_r i.e. $[\sigma_r]_1$ is obtained. The first approximation of stress ratio, i.e. $[x]_1$, is obtained by dividing $[\sigma_r]_1$ by σ_θ which can be substituted in Eq. (11) to calculate first approximation of $\phi(r)$ i.e. $[\phi\,(r)]_1$. Now one carries out the numerical integration of $[\phi(r)]_1$ from limits of a to r and uses this value in Eq.(14) to obtain first approximation of $\psi(r)$ i.e. $[\psi\,(r)]_1$ Using this $[\psi\,(r)]_1$, in Eq. (16) and (17) respectively, $[\psi_1(r)]_1$ are found, which are used in Eq. (15) to find second approximation of σ_θ i.e. $[\sigma_\theta]_2$. Using $[\sigma_\theta]_2$ for σ_θ in Eq. (22), second

ISSN 2229-5518

approximation of σ_r i.e. $[\sigma_r]_2$ is found and then the second approximation of x ie. $[x]_2$ is obtained.

LEGENDS:

ITER = Iteration no
h = Limiting value of Err (=0.01)
ITM = Maximum no of iterations

$$\mathrm{ERR} = \frac{[\sigma_\theta(r)]_{\mathrm{ITER}} - [\sigma_\theta(r)]_{\mathrm{ITER-1}}}{[\sigma]_{\mathrm{ITER-1}}}$$

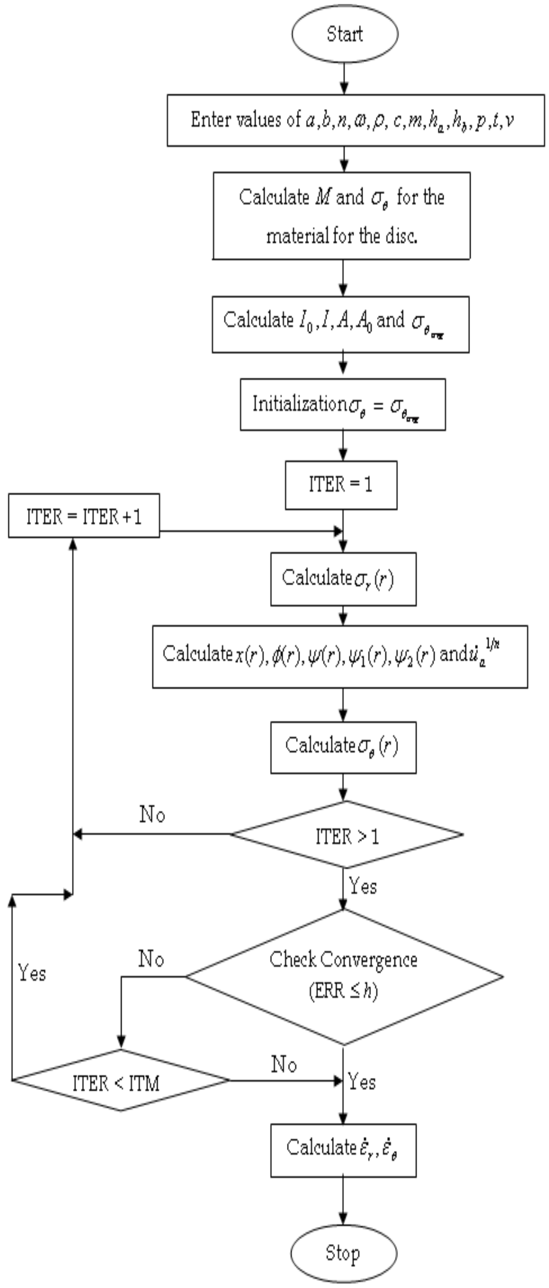

Figure 2. Numerical scheme of computation.

The iteration is continued till the process converges and gives the values of stresses at different points of the radius grid.

For rapid convergence 75 percent of the value of σ_θ obtained in the current iteration has been mixed with 25 percent of the value of σ_θ obtained in the last iteration for use in the next iteration i.e $\sigma_{\theta\,next} = .25\sigma_{\theta\,previous} + .75\sigma_{\theta\,current}$. The strain rates are then calculated now from the Equations (8), (9) and (10).

7. ANISOTROPIC CONSTANTS AND NUMERICAL COMPUTATIONS

For the sake of computation, we have chosen material parameters as particle size $P = 1.7\,\mu m$, particle content $V = 30\%$ and temperature $T = 623\,K$ as reported in Pandey *et al*.[10]. The stress exponent and Density of disc material have been taken as $n = 8$ and $\rho = 2862.1 kg/m^3$. The inner radii a and the outer radii b of all the discs are taken as 31.75 mm and 152.4 mm respectively. The anisotropic constants have been taken from [7] and the numerical results have been calculated for two cases of anisotropy each deviating from isotropy. The remaining two cases of anisotropy are almost similar and hence they have been omitted for computational purpose.

Table 1: Anisotropic Constants

	Case 1	Case 2	Case 3	Case 4	Case 5
G/F	.8159	1.200	1.000	.7452	1.34
H/F	.6081	.7452	1.000	1.2200	1.64

8. EFFECT OF DISC PROFILE ON ANISOTROPIC DISC

The effects of varying the disc thickness on creep behavior of composite disc made of anisotropic material (6061Al - *30%* vol SiC_p) are shown in Figures 8.1 – 8.4. These graphs show the variation in stresses and strain rates. In disc for anisotropic material, the thickness have been taken as $h_a = 1.0\text{mm}$ to $h_b = 1.0\text{mm}$ (Constantly), $h_a = 1.44\text{mm}$ to $h_b = 0.75\text{mm}$ (Linearly) and $h_a = 2.42\text{mm}$ to $h_b = 0.76\text{mm}$ (Hyperbolically)

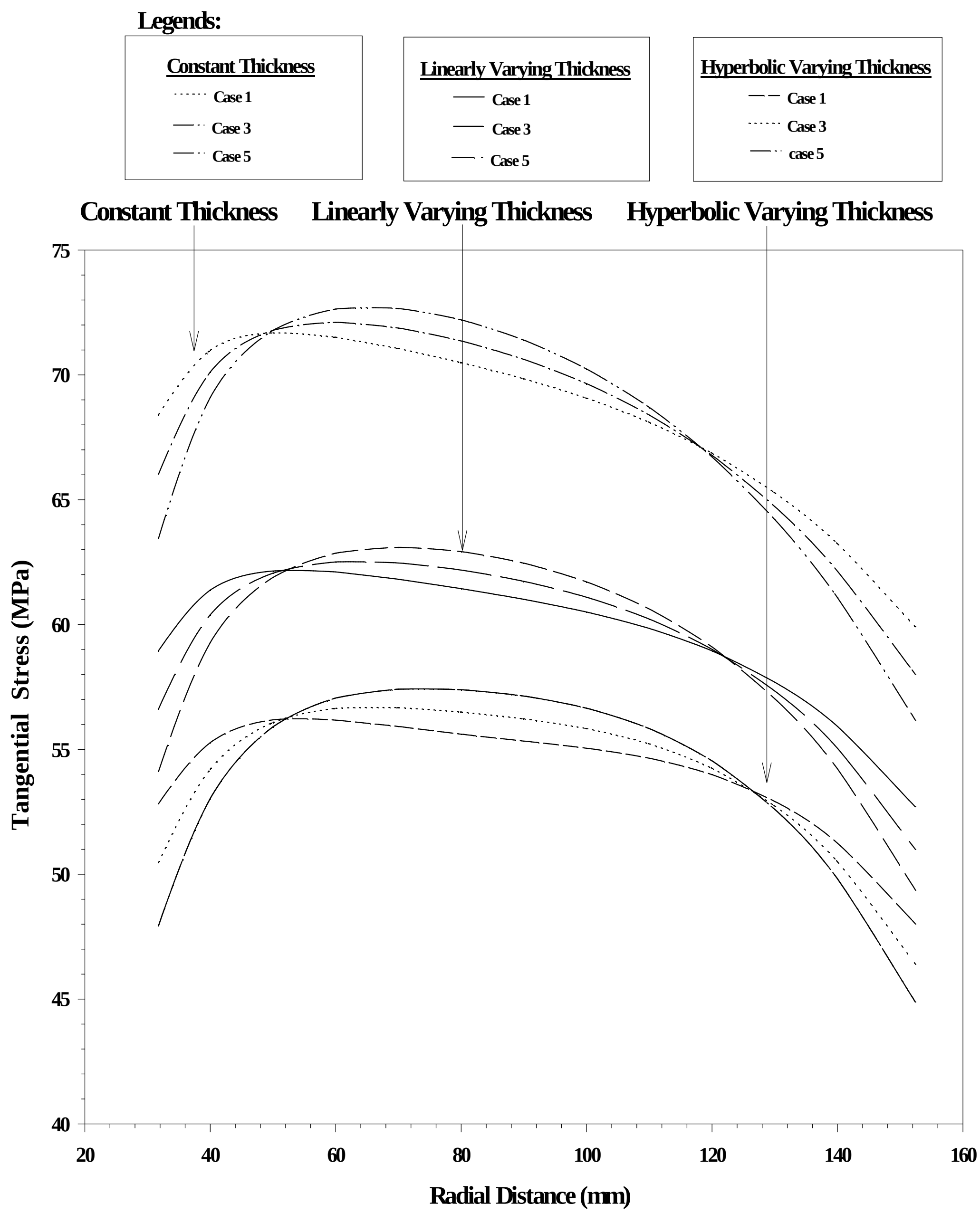

Figure 8.1 Variation of tangential Stress along the radial distance of the discs rotating with an angular velocity 15000 rpm at 623K.

Figure 8.1 shows the variation of tangential stress in a rotating disc along the radius in the disc for two different cases of anisotropy and three thickness profiles. The tangential stress in the inner and outer part of disc is lowest in case 5 and highest in case 1, while it lies in between the two in case 3. In the middle part of the disc, the tangential stress is lowest in case 1 and highest in case 5, while it lies in between the two in case 3. The trend of variation of tangential stress is similar in all cases of thickness profile variations. The tangential stress in anisotropic rotating disc having hyperbolic thickness is reduced everywhere compared to disc of uniform thickness and linearly varying thickness.

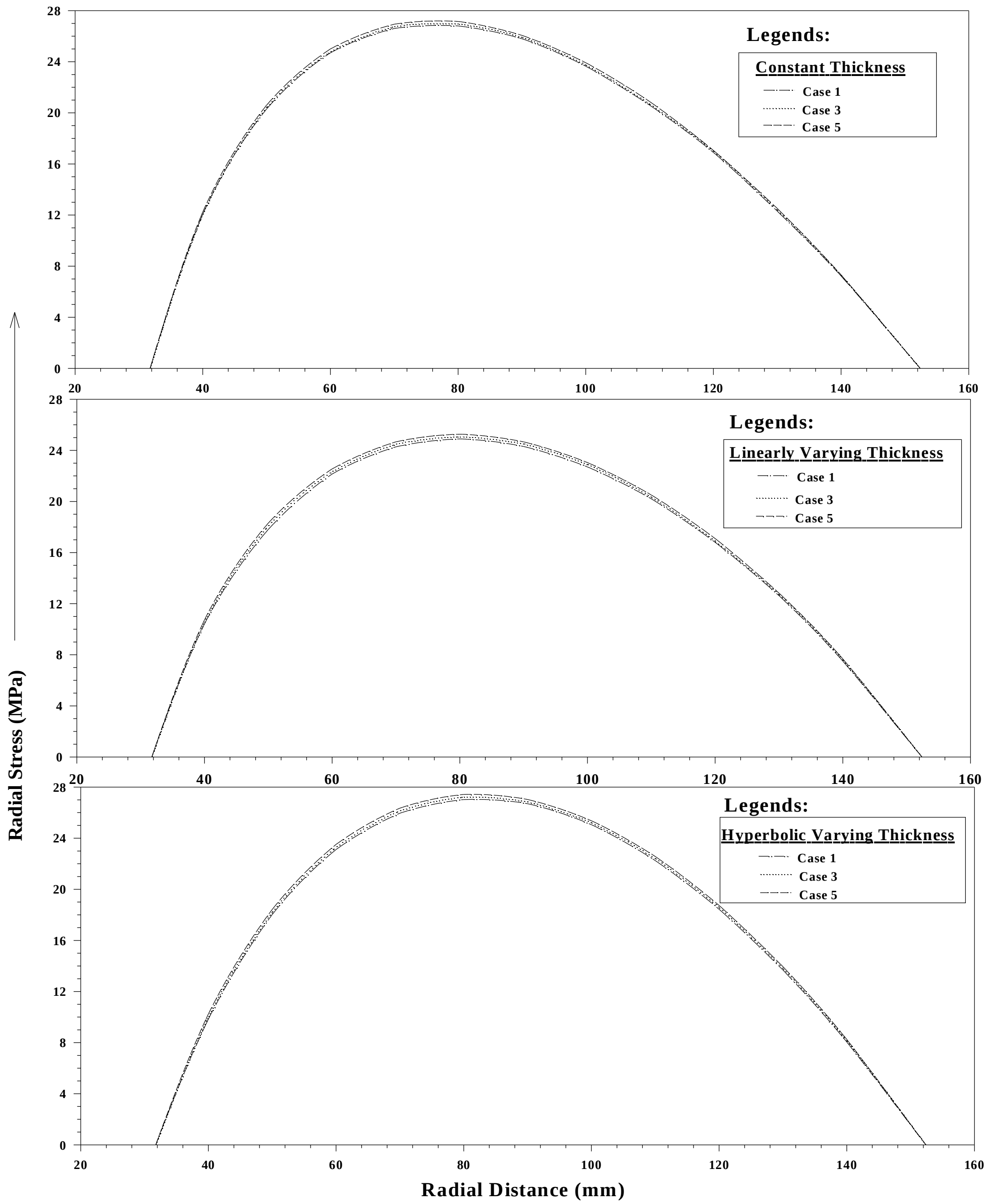

Figure 8.2 Variation of radial stress in rotating discs along the radius of the disc rotating with an angular velocity 15000 rpm at 623K.

Figure 8.2 shows the variation of the radial stress in rotating disc along the radius of the disc. The radial stress is not much affected by introducing anisotropy in the disc as the values of radial stress are very close for all the different cases of anisotropic constants and the effect of disc profile on radial stress is similar to disc made of isotropic composite. The disc having hyperbolically varying thickness has lower radial stress than uniform thickness disc, but litter higher than the disc with linearly varying thickness near the inner radius of disc, but towards the outer radius the radial stress is the highest.

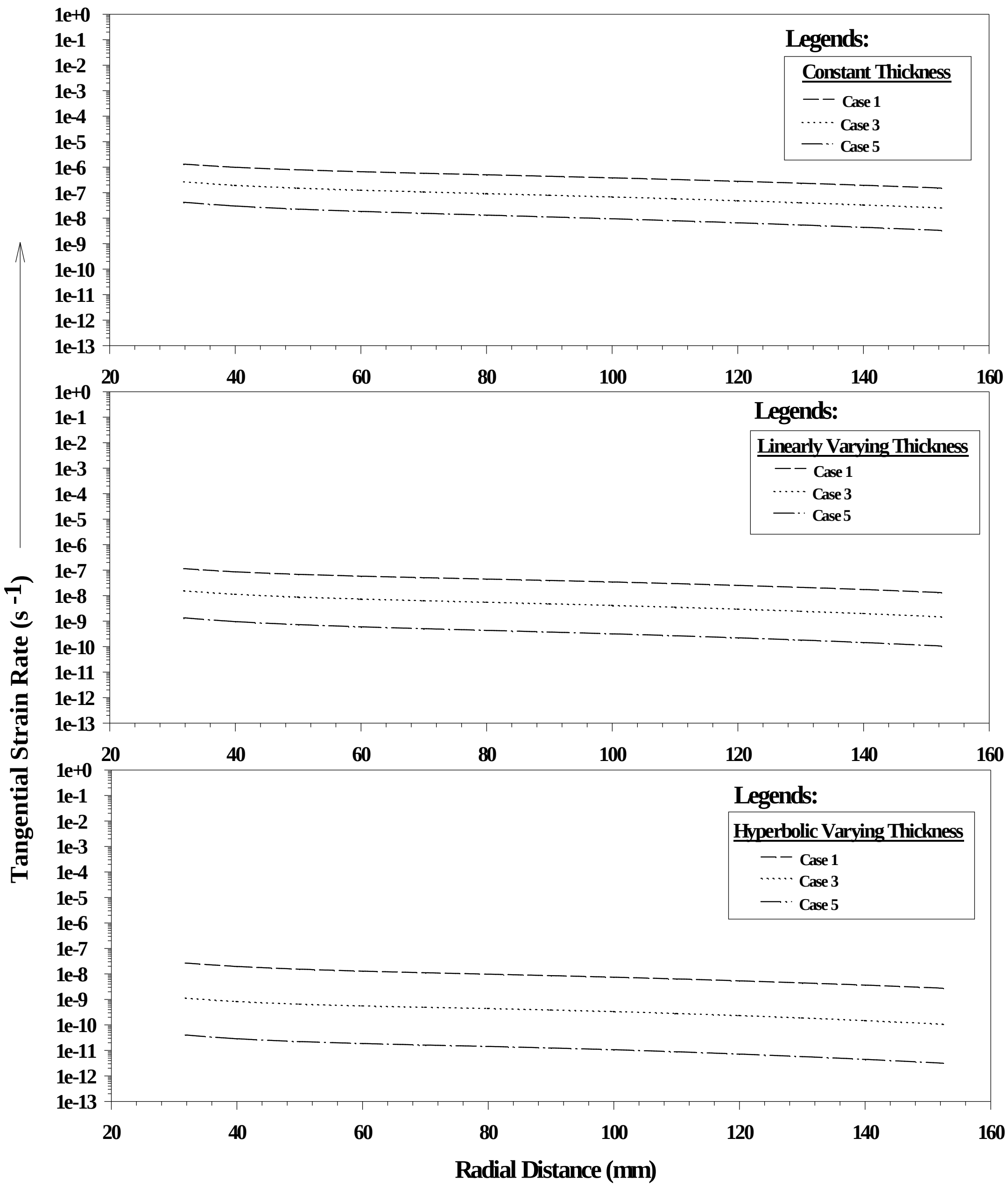

Figure 8.3 Variation of tangential strain rate along the radial distance of the disc rotating with an angular velocity 15000 rpm at 623K.

Figure 8.3 shows that the variation of tangential strain rate along the radius of the disc. In all the cases of thickness variations, the tangential strain rate is highest at the inner disc and then decreases continuously when one moves towards the outer disc. In all cases of thickness profile variation, the tangential strain rate is maximum in the case 1 of anisotropy and minimum in the case 5 of anisotropy. The values of tangential strain rate in case 3 of anisotropy always lie between these two. Therefore the anisotropy of type 5 helps to decrease the tangential strain rate. In case of hyperbolic variation of thickness of the disc, the tangential strain rate is relatively less compared to the strain rate in other two variations in the thickness of the disc. Thus the combination of anisotropic of type 5 with hyperbolic varying thickness yields less tangential strain rate.

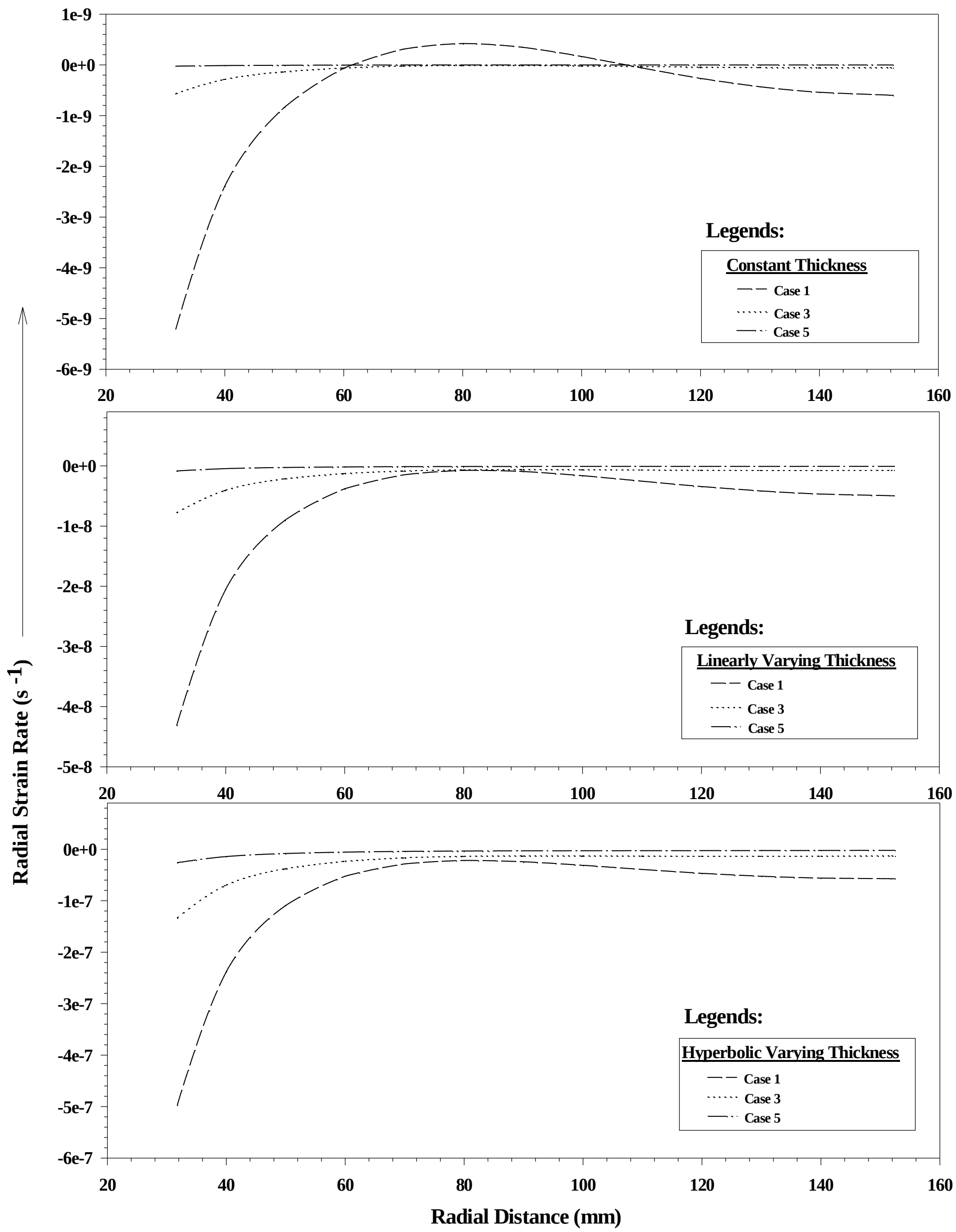

Figure 8.4 Variation of radial strain rate along the radial distance of the discs rotating with an angular velocity 15000 rpm at 623K

Figure 8.4 shows the variation of radial strain rate along the radius of the disc. For the material of anisotropy of type 1, the compressive radial strain rate is maximum in inner radius and goes on decreasing up to a certain radial distance followed by an increasing trend towards the outer radius. The nature of radial strain rate which is compressive to tensile at the middle of the disc for cases 1, whereas for cases 3 and 5, the compressive radial strain rate decreases continuously from inner radius towards outer radius. The radial strain is also less if one selects the anisotropy of type 5 with hyperbolic variation in the disc.

10. CONCLUSION

The above results and discussion concludes that

1. The anisotropy of material helps in restraining the creep in the rotating disc.
2. Since the ratios of anisotropic constants basically depend upon tensile and compressive yield stresses of the composite, the care should be taken to introduce anisotropy.
3. The anisotropy of type 5 seems justified for the safe design of the disc as in this case the nature of the radial strain rate does not change and it is compressive for all the cases of thickness profile variation.
4. By taking the anisotropy of type 5 with hyperbolic thickness, the magnitude of tangential creep rate is reduced by about four order of magnitude compared to those for isotropic composites with constant thickness.
5. The radial strain rate is also reduced significantly for hyperbolic profile and anisotropy of type 5.

NOMENCLATURE:

a	Inner radius of disc (31.75 mm)	b	Outer radius of disc (152.4mm)
$\|b_r\|$	Magnitude of burgers vector	D_L	Lattice diffusivity
$\dot{\bar{\varepsilon}}$	Effective strain rate (s^{-1})	$\bar{\sigma}$	Effective stress (*MPa*)
r	Radius of disc	T	Temperature (K)
E	Young's modulus	h	Thickness of disc (mm)
ρ	Density of composite	λ	Subrain size
m	Creep parameters	σ_θ	Tangential and radial stress (MPa)
$\dot{\varepsilon}_\theta$, $\dot{\varepsilon}_r$	Tangential and radial strain rates (s^{-1})	$x(r)$	The ratio of radial to tangential stress at any radius (r)
F, G, H	Hill's anisotropic constants	ω	Angular velocity of disc (=15000 radian / sec)
$\sigma_{\theta_{avg}}$	Average tangential stress over cross section of the disc	σ_0	Threshold stress

REFERENCES

[1] Wahl, A.M., Sankey, G.O., Manjoine, M.J. and Shoemaker, E. Creep tests of rotating risks at elevated temperature and comparison with theory. Journal of Applied Mechanics, 76, 225-235 (1954).

[2] Ma, B.M. A Creep Analysis of Rotating Solid Discs. J .of the Franklin inst, 267 (2), 167-168, (1959).

[3] Ma, B.M. A further creep analysis for rotating solid disks of variable thickness. Journal of the Franklin Institute, 269, 408-419 (1960).

[4] Sherby, O.D., Klundt, R. H. and Miller, A. K. Flow stress, subgrain size and subgrain stability at elevated temperature. Metallurgical Transactions, 8A, 843-850 (1977).

[5] Arya, V.K. and Bhatnagar, N.S. Creep analysis of rotating orthotropic disc. Nuclear Engineering and Design, 55, 323 (1979).

[6] Nieh, T.G. Creep rupture of a silicon carbide reinforced aluminum composite. Metallurgical Transactions, 15A, 139-146 (1984).

[7] Kulkarni, P.S., Bhatnagar, N.S. and Arya, V.K. Creep analysis of thin-walled anisotropic cylinders subjected to internal pressure, bending and twisting. Proceedings of the workshop on solid mechanics, 13-16 (1985).

[8] Bialkiewicz, J. Dynamic Creep Rupture of a Rotating disc of Variable Thickness. International Journal of Mechenical Science, 28 (10), 671-681 (1986).

[9] Bhatnagar, N.S., Kulkarni, P.S. and Arya, V.K. Steady State Creep of Orthotropic Rotating Discs of Variable Thickness. Nuclear Engineering and Design, 91, 121-141 (1986).

[10] Pandey, A.B., Mishra, R.S. and Mahajan, Y.R. Steady State Creep Behaviour of Silicon Carbide Particulate Reinforced Aluminium Composites. Acta. Metallurgica Materialia., 40(8), 2045-2052 (1992).

[11] Gupta, S.K., Sharma, S and Pathak, S. Creep transition in a thin rotating disc having variable thickness and variable density. Indian Journal of Pure applied Math., 31(10), 1235-1248 (2000).

[12] Singh, S.B. and Ray, S. Modeling the anisotropy and creep in orthotropic Al-SiC composite rotating disc. Mechanics of Materials, 34, 363-372 (2002).

[13] Orcan, Y. and Eraslan, A.N. Elastic-plastic stresses in linearly hardening rotating solid disks of variable thickness. Mechanics Research Communications, 29, 269-281 (2002).

[14] Gupta, V.K. Steady state creep and material parameters in a rotating disc of Al-SiCp composite. European Journal of Mechanics A/Solids, 23, 335-344 (2004).

[15] Jahed, H., Farshi, B. and Bidabadi, J. Minimum weight design of inhomogeneous rotating discs. International Journal of Pressure Vessels and Piping, 82, 35-41 (2005).

[16] Baykara, C. A comparison of stress concentrations in thin sheetswith plastic anisotropy. Journal of Reinforced Plastics and Composites, 26, 1455-1459 (2007).

[17] Singh, S.B. One parameter model for creep in a whisker reinforced anisotropic rotating disc of Al-SiCw composite. European Journal of Mechanics A/Solids, 27(4), 680-690 (2008).

[18] Rattan, M., Singh, S. B and Ray, S. Effect of stress exponent of steady state creep in an isotropic rotating disc. Bulletin of Calcutta Mathematical Society, 101 (2009).

[19] Chamoli, N., Rattan, M. and Singh, S.B. Effect of anisotropy on the creep of a rotating disc of Al-SiCp composite. Indian Journal of Contemp. Math. Sciences, 5(11), 509 –516 (2010).